Polaronic effects in TiO_2 calculated by the HSE06 hybrid functional: Dopant passivation by carrier self-trapping

Peter Deák,* Bálint Aradi, and Thomas Frauenheim
Bremen Center for Computational Materials Science, University of Bremen, P.O. Box 330440, D-28334 Bremen, Germany
(Received 26 November 2010; revised manuscript received 19 January 2011; published 19 April 2011)

Metal oxides are extremely challenging for defect calculations within density-functional theory because of the underestimation of the band gap and of the polaronic effects due to spurious electron self-interaction in the standard (semi)local implementations. We show here that—similarly to Group-IV semiconductors—the HSE06 screened hybrid functional provides not only a good description of the ground-state properties and an accurate gap of TiO_2 modifications, but fulfills the generalized Koopmans' theorem for host-related defect states—independent of localization. This means that the total energy has the correct dependence on the fractional occupation number, lending credibility to the calculated optical and thermodynamic charge transition levels for acceptors (Al, Ga, In, Sc, and Y on Ti site) and donors (Nb on Ti site, and interstitial H). We find deep, localized hole polarons in anatase and electron polarons in rutile. Therefore, *p*-type doping in anatase and *n*-type doping in rutile are counteracted by carrier self-trapping. Donors in anatase and the acceptors in rutile give rise to effective masslike states, but the latter are deeper. In fact, the polaron bound at In in anatase is about as deep as the effective masslike state induced by In in rutile. The shallow state in anatase and the deep one in rutile for the Nb donor, as well as the deep state for Al in anatase, agree well with experimental observations.

DOI: 10.1103/PhysRevB.83.155207 PACS number(s): 71.55.Ht, 71.38.−k, 71.20.Ps, 71.15.Mb

I. INTRODUCTION

Metal oxides are a challenge for the "standard toolkit" of defect calculations: density-functional theory (DFT) applied to supercells.[1] The underestimation of the band gap by the local-density approximation (LDA) and the semilocal generalized gradient approximation (GGA) in these systems is often very serious, and defect levels, which are observed in the gap, appear as resonances in the calculated bands, leading to a qualitatively wrong description of the defect behavior.[1–4] The reduced screening in these ionic systems makes the electron self-interaction error and the orbital-dependent exchange effects also more apparent. Particularly, polaron localization is strongly suppressed.[5] Recently, a correction scheme, based on parametrized nonlocal potentials and acting only on host-derived defect states, has been suggested.[6] The parameters have been set to ensure the equality between the Kohn-Sham (KS) energy level of the defect and the electron addition and/or subtraction energy. This so-called generalized Koopmans' theorem (gKT), which is increasingly being used for setting empirical parameters[7] or to test the reliability of a method,[8] follows from Janak's theorem and is an attribute of the exact DFT functional,[9] for which the total energy is a linear function of the fractional occupation numbers. It was noted that, because in Hartree-Fock (HF) theory this function is concave, while in (semi)local approximations of DFT it is convex, hybrid functionals (mixing HF and GGA exchange) may recover the correct behavior.[6] Screened[10] and hybrid-exchange functionals[11–13] nowadays gain increasing acceptance in defects studies, due to their better ability to reproduce the bulk band gap.[14] The screened hybrid functional of Heyd, Scuseria, and Ernzerhof (HSE06)[11] was shown to be particularly successful in describing not just the band gap but also the ground-state properties of a whole range of materials,[15] using a fixed HF:GGAmixing ratio of 25 : 75 and a screening parameter of 0.2 $Å^{-1}$. In some systems, tuning of the mixing parameter seemed to be necessary, though.[4,16] It is also not obvious that a mixing parameter, which provides optimal ground-state properties and band gap, will also be optimal for fulfillment of the gKT.[6] Recently, we have shown[17] that HSE06 reproduces the ground-state properties and band gap of Group-IV semiconductors very well, and for host-derived donor and acceptor states the gKT is fulfilled within 0.1 eV, independent of the level position in the gap. The calculated charge transition levels were also in excellent agreement with experiment.[17] In this paper we show that the gKT is satisfied well in TiO_2, and HSE06 also describes polaronic effects correctly. Therefore, HSE06 can be used to tackle defect-related problems in TiO_2.

TiO_2 is a widely used photocatalytic material with many potential application in electronics, optoelectronics, and photovoltaics, most of which relying on the control of free-carrier generation, transport, and recombination.[18] Theoretical studies of electrically active defects in TiO_2 are, therefore, of great importance, but the lack of correct reproduction of the polaronic effects has been hampering a useful contribution of theory. For example, Nb in anatase gives rise to a shallow effective masslike (EMT) donor state, turning the crystal into a transparent conducting oxide at high concentrations,[19,20] whereas rutile, doped with Nb to similar concentrations, remains isolating due to a deep level in the gap.[21,22] GGA predicts EMT donors states,[23] whereas a GGA + U calculation resulted in deep polaronic states in both modifications.[24] (It should be noted, though, that another GGA + U study gave an EMT state for Nb in anatase.[25]) The hybrid B3LYP functional on a localized basis resulted in two possible defect configurations with almost the same energy for Nb in anatase: one with a shallow state and one with a deep state.[26] Similar problems have been encountered with other donor-type defects, such as the oxygen vacancy and the hydrogen interstitial.[27,28] By

applying HSE06, we find (in agreement with experiments on Nb-doped samples) that polaronic electron states (self-trapping of the donor electron) only occur in rutile, while both Nb on Ti site (Nb_{Ti}) and interstitial H (H_i) give rise to EMT states in anatase.

The *p*-type doping of TiO_2 is important mainly in band-gap engineering for visible-light photocatalysis,[29] but it would be of interest for displays, solar cells, and transparent electronics as well. So far most studies have concentrated on nitrogen[30–32] and carbon,[32,33] substituted on the anion site. It has been long known that Al on the cation site is also an acceptor, diminishing catalytic activity related to mobile electrons.[34] Its electronic properties have been theoretically investigated in both rutile and anatase.[35–38] GGA calculations in anatase[38] predict aluminum to be a shallow acceptor with a delocalized hole state, while calculations with a PBE0 hybrid (defined as the mixing of 75% GGA exchange, calculated with the Perdew-Burke-Ernzerhoff functional, and 25% HF exchange) in rutile[38] and HF calculations in both rutile and anatase[38] show an Al-bound hole polaron with an acceptor level above migap. To our knowledge, other potential single acceptors, like Ga, In, Sc, and Y on a cation site have not yet been considered. By investigating several acceptors in TiO_2 by HSE06 we find (in agreement with experiments on Al-doped samples) that polaronic hole states (self-trapping of the acceptor hole) occur only in anatase, while all investigated cation site acceptors have EMT states in rutile.

II. METHOD OF CALCULATION

Calculations have been carried out with the Vienna *ab initio* simulation package, VASP 5.2.8, using the projector augmented wave (PAW) method.[39] The following cores have been used: O:(He), Al:(Ne), Sc:(Ne), Ti:(Ne,$3s^2$), Ga:(Ar), Y:(Ar,$3d^{10}$), Nb:(Ar,$3d^{10}$,$4s^2$), and In:(Kr). Bulk properties have been calculated in the primitive cells with an 8×8×8 Monkhorst-Pack (MP) set,[40] reduced by a factor of 2 in the Fock-exchange part.[41] Convergence of the total energy has been achieved by setting the plane-wave cutoff for the wave-function expansion (and for that of the charge density) to 420 (840) eV. Geometries were relaxed with a maximal force criterion of 0.02 eV/Å. Defect calculations have been carried out with the same cutoffs on an anatase supercell of 96 atoms ($2\sqrt{2} \times 2\sqrt{2} \times 1$times the Bravais cell) and on a rutile supercell of 72 atoms (2×2×3 primitive cells). The latter is rather small, but HSE06 calculations on larger systems with this basis are not yet possible for us due to the much too long computing times. Therefore, one test has been carried out for a 192-atom ($2\sqrt{2} \times 2\sqrt{2} \times 4$) cell, using the larger Ti(Ar) core but with cell parameters determined by the smaller one. For supercell calculations the Γ-point approximation and a 2×2×2 non-Γ-centered MP set was used.

The fulfillment of the gKT can be checked by comparing the position of the *vertical* charge transition level, ΔE^v, to that of the KS defect level [see, e.g., Fig. 1 in Ref. 17]. The former is the difference between the total energy of the relaxed neutral defect, E_0(geom:0), and of the ionized defect in the geometry of the neutral one, E_q(geom:0):

$$\Delta E^v = [E_q(\text{geom} : 0) - E_0(\text{geom} : 0)]/q. \quad (1)$$

Therefore, the vertical charge transition does not contain the energy of ionic relaxation after the ionization. That is included in the *adiabatic* transition level, ΔE^a, which is the difference between the total energies of the neutral and the ionized defects, both being calculated in their equilibrium geometry.

$$\Delta E^a = [E_q(\text{geom} :q) - E_0(\text{geom} :0)]/q. \quad (2)$$

Note that ΔE^v is the relevant quantity for, e.g., photoelectron spectroscopy, while ΔE^a is measured, e.g., in deep-level transient spectroscopy. For the defect-related KS levels, calculated at the equilibrium geometry of the neutral defect, we will use the notation ε_h and ε_e, where ε_h is understood as the empty defect level of the neutral acceptor or the positive donor, while ε_e is the occupied defect level of the negative acceptor or the neutral donor. The position of both the charge transition level and the KS levels is taken with respect to the band edge of the perfect crystal: to the valence band for acceptors and to the conduction band for donors (after proper potential alignment).

For checking the fulfillment of the gKT in the vertical charge transitions of the defects, the Γ-point approximation (1×1×1 MP set) was used. Convergence of the adiabatic transition levels were tested with a 2×2×2 non-Γ-centered MP set. The average potentials between the perfect crystal and the defective supercell have been aligned using the method suggested in Ref. 2. For geometry optimization the same force criterion was used as in the case of the unit cells. Charged supercells were calculated assuming a jellium charge of opposite sign, which requires correction to the total energy as well as to the KS levels. The procedures suggested in Refs. 2,3, and 6 were applied. (Because our supercells are nearly cubic, and the dielectric constant $\varepsilon \gg 1$, the full correction to the total energy was taken as 65% of the monopole correction.) For vertical transitions, the geometric average of the longitudinal and transversal *electronic* dielectric constants of Ref. 42 was used in the charge correction. In case of the adiabatic transition, where the *static* dielectric constant is needed, the situation is more problematic. On the one hand, the ionic part of the dielectric constant is much more anisotropic than the electronic part. On the other, even though the experimental static constants are quite large (negligible correction), calculations on such relatively small supercells severely underestimate them. (It is also probable that such a high concentration of defects modifies the dielectric constant.) Because, however, the fulfillment of the gKT can already be proven at the vertical transitions, we will circumvent the problem of the charge correction in the case of the adiabatic transitions by adding the relaxation energy in the ionized state to the vertical ionization energy:

$$\Delta E^a = \Delta E^v + [E_q(\text{geom} :q) - E_q(\text{geom} :0)]. \quad (3)$$

The vertical ionization energy, ΔE^v, is replaced by the KS level in the neutral state of the defect (no need for charge correction). Because the expression in the parentheses refers to total energies in the same charge state, the errors due to the lack of charge correction are expected to be canceled.

TABLE I. Lattice constants (a,c in Å), band gap (E_g), and valence band (VB) width (in eV) of TiO_2.

	LDA[a]	HSE06	G_0W_0[b]	Experiment
Anatase				
a	3.744	3.755		3.782[c]
c	9.497	9.561		9.502[c]
u	0.207	0.207		0.208[c]
E_g	2.05	3.58	3.56	3.420[d]
VB width	5.0	4.5		4.7[f]
Rutile				
a	4.555	4.567		4.587[c]
c	2.922	2.944		2.954[c]
u	0.304	0.305		0.305[c]
E_g	1.88	3.37	3.34	3.035[e]
VB width	6.0	6.4		6.5[g]

[a]Reference 44.
[b]Reference 45.
[c]Reference 52, and references therein.
[d]Reference 53.
[e]Reference 54.
[f]Reference 55.
[g]Reference 50.

III. RESULTS AND DISCUSSION

According to Table I, the lattice parameters of TiO_2, as obtained by HSE06,[43] show a slight improvement over the LDA ones[44] when compared to experiment. However, in contrast to the strong underestimation in LDA, HSE06 results in a direct band gap of 3.37 eV for rutile, and an indirect ($0.85\Delta \rightarrow \Gamma$) band gap of 3.58 eV for anatase, in excellent agreement with the results of a recent full frequency-dependent G_0W_0 calculation.[45] Note that, in accord with other G_0W_0 calculations,[46–48] the quasi-particle band gaps are higher[49] than the ones found in optical experiments, but for rutile are in good agreement with photoelectron spectroscopy results.[50] Because, according to experience, G_0W_0 is a good approximation to self-consistent GW with vertex correction, and because the solution of the Bethe-Salpeter equations did not diminish the gap, it was speculated that the deviation from experiment is due to electron-phonon coupling in the optical transitions.[45] This is not included in the HSE06 calculation either, so the result for the gap can be regarded as excellent. As for Group-IV semiconductors,[17] not just the band gap improves with HSE06 but also the valence band width. We note that the full density of states (DOS) calculated by HSE06 agrees very well with the G_0W_0 results of Ref. 45 for rutile, and with photoelectron spectra for both modifications.[51]

In Table II we compare the KS levels of the hole and electron states of the defects to the electron addition and subtraction energy, respectively, at a fixed geometry. With respect to the band edges, these energies provide the vertical (or optical) charge transition levels.[56] In checking the fulfillment of the gKT, one has to take into account the inaccuracy of the simplified charge correction schemes for levels and total energies. The most accurate prediction is expected from the KS level of the defect in the neutral charge state (ε_h for acceptors and ε_e for donors; boldface numbers in Table II), which does not contain charge correction at all. The error of the charge

TABLE II. KS eigenvalue of the defect-related hole and electron levels, as well as the vertical charge transition, ΔE^v, calculated in the Γ approximation. (All values in eV, with respect to the valence band edge for acceptors and to the conduction band for donors.) ε_h for acceptors and ε_e for donors refer to the neutral charge state and contain no charge correction.

	ε_h	ε_e	ΔE^v
Anatase: Al_{Ti}	**+2.17**	+2.20	+2.22
Anatase: Ga_{Ti}	**+2.03**	+2.02	+2.02
Anatase: In_{Ti}	**+1.69**	+1.73	+1.85
Anatase: Sc_{Ti}	**+1.71**	+1.72	+1.75
Anatase: Y_{Ti}	**+2.40**	+2.21	+2.33
Anatase: Nb_{Ti}	−0.48	**−0.33**	−0.39
Anatase: H_i	−0.42	**−0.27**	−0.33
Rutile: Al_{Ti}	**+0.46**	+0.54	+0.41
Rutile: Ga_{Ti}	**+0.45**	+0.52	+0.33
Rutile: In_{Ti}	**+0.44**	+0.49	+0.53
Rutile: Nb_{Ti}	−1.02	**−1.02**	−0.86
Rutile: H_i	−1.00	**−1.00**	−0.82

corrections is difficult to estimate but is certainly larger than in the case of Group-IV elements (with truly cubic lattices and stronger screening). Certainly, the error of the simple corrections varies with the localization of the defect-related wave function and the charge distribution,[57] and it is not the same for the KS level of the charged system and for the total energy difference. Considering these uncertainties, the agreements with the reference neutral KS values is quite good (within 0.2 eV), and the deviations are not bigger than the example cases quoted for GW calculations in Ref. 8. We note that in an HSE study on rutile,[4] Janotti *et al*. has suggested to diminish the HF fraction to 0.20, in order to reproduce the low-temperature optical band gap. As outlined at the beginning of this section, we do not believe that such a fitting is necessary. In fact, with 0.2 HF fraction, the lattice parameters improve very slightly, but the gKT is not any better satisfied: e.g., in the case of H_i, ε_h, ε_e, and ΔE become −0.91, −0.68, and −0.64 eV, respectively.

Our HSE06 results show an interesting trend: acceptor states are very deep and donor states shallower in anatase, while the opposite occurs in rutile. (Note that H_i in both modifications forms an OH group, as found earlier.[28,58,59]) Plots of the defect wave functions show that all the acceptors considered in anatase introduce small hole-polaron states. According to Fig. 1, the hole provided by the acceptor is trapped by an oxygen first neighbor in the case of the deeper Al and Ga and of the somewhat shallower In and Sc (Ga and Sc not shown) as well, while in case of Y it is localized mostly on an oxygen second neighbor. One could consider these defects as a complex of a negatively charged acceptor and a host oxygen atom which has undergone a (2−/−) charge transition (i.e., acting as a donor). In contrast, the donors Nb_{Ti} and H_i give rise to completely delocalized EMT states in anatase, with similar level positions.

In rutile all investigated acceptors have a delocalized EMT hole state, again with similar level positions. However, the donors, Nb_{Ti} and H_i, both provide deep states. A plot of the

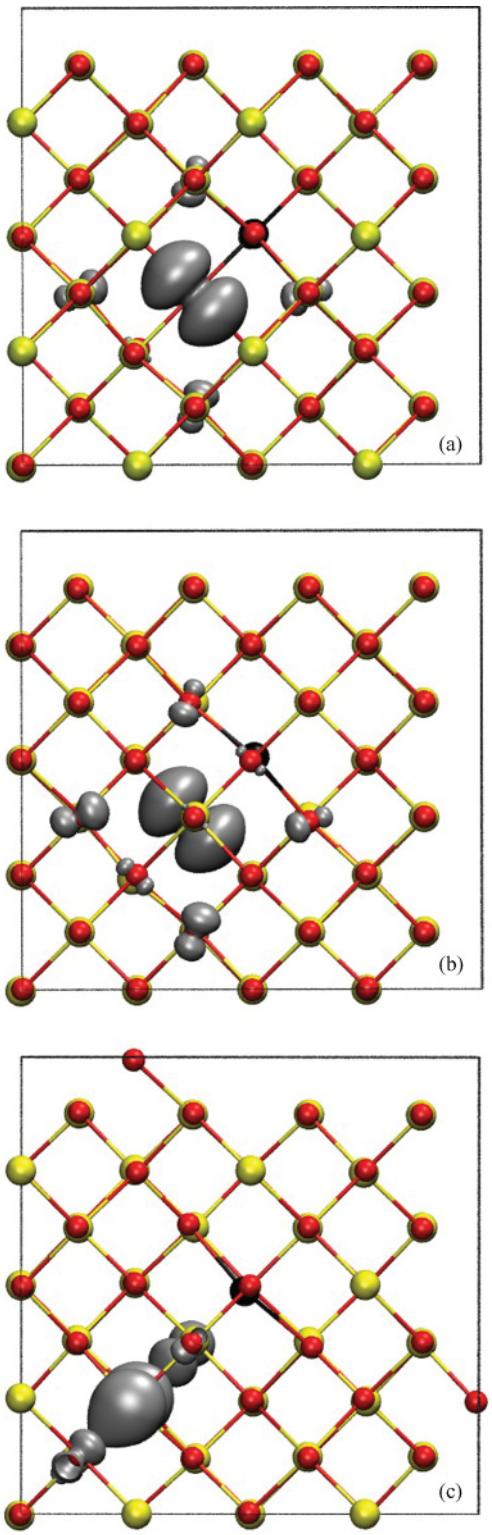

FIG. 1. (Color online) The hole state of the (nominally) neutral acceptors, Al (a), In (b), and Y (c) in anatase. Ti and O atoms are large light (yellow in color) and small dark (red in color) spheres, respectively. The dopant is the large dark (black in color) sphere in the center. The isosurface was plotted at 0.023 e/Å^3.

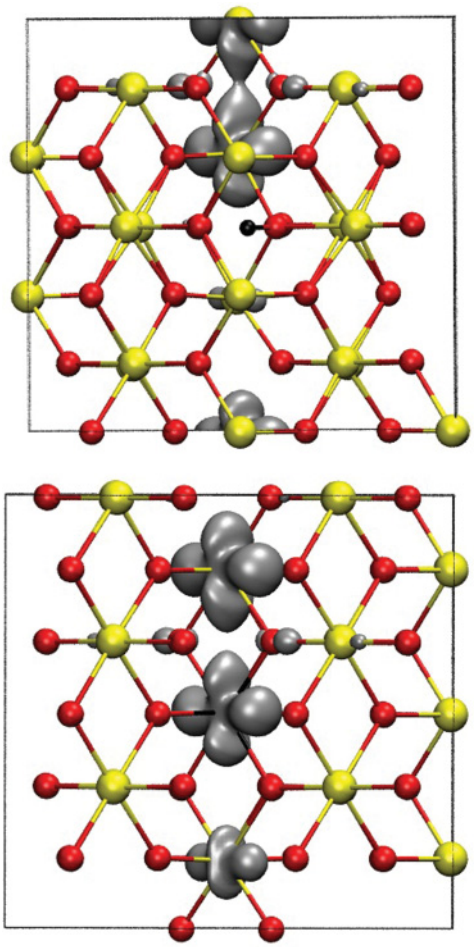

FIG. 2. (Color online) The electron state in the case of the (nominally) neutral donors H_i (a) and Nb_{Ti} (b), in a 72-atom rutile supercell. The isosurface was plotted at the value of 0.027 e/Å^3.

wave functions (Fig. 2) in the rather small 72-atom cell show that two Ti neighbors give significant contribution (in the case of Nb_{Ti} also the dopant itself), but the calculation on H_i in a 192-atom cell (with larger core) shows, in Fig. 3, that to be a size effect. The main contribution comes really from just one

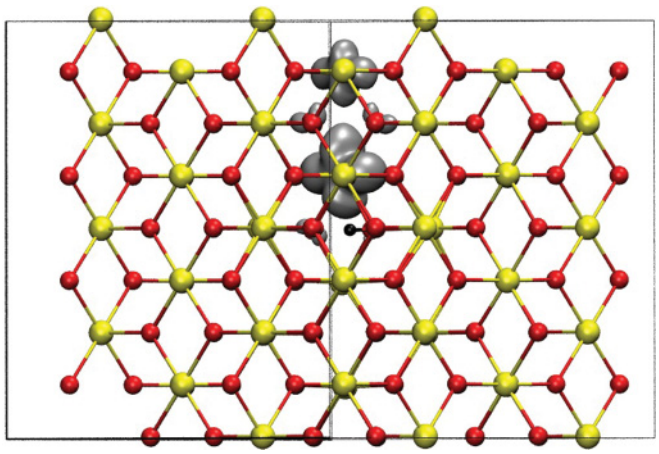

FIG. 3. (Color online) The electron state of the H_i donor in a 192-atom rutile supercell.

TABLE III. Adiabatic charge transition levels, ΔE^a, in anatase (A) and rutile (R). (All values in eV, with respect to the valence band edge for acceptors and to the conduction band for the donor.) Convergence against MP set has been checked for the acceptors Al and In, and the donors Nb and H. The effect of cell size was tested for H_i in rutile using a large core for Ti (values given in parentheses).

	Al	Ga	In	Sc	Y	Nb	H
A-96 1×1×1	+0.9	+0.8	+0.6	+0.6	+0.9	−0.3	−0.3
A-96 2×2×2	+0.8		+0.6			−0.3	−0.2
R-72 1×1×1	+0.5	+0.4	+0.4			−0.8	−0.6 (−0.5)
R-72 2×2×2	+0.4		+0.6			−0.7	−0.5
R-192 1×1×1							(−0.7)

TABLE IV. Heat of formation (eV) of the neutral acceptor defects of TiO_2 for values of the oxygen chemical potential, ranging from that in the O_2 molecule (extreme oxygen rich) to that in Ti_2O_3 (oxygen poor). The values were obtained for 96-atom anatase (A) supercells in the Gamma approximation, and for 72-atom rutile (R) supercells with a 2×2×2 MP set.

Anatase	Al	Ga	In	Sc	Y
O rich (Ti poor)	1.7	2.3	2.9	2.3	3.3
Stoichiometric	2.9	3.5	4.1	3.6	4.5
O poor(Ti rich)	3.6	4.2	4.8	4.2	5.2
Rutile	**Al**	**Ga**	**In**		
O rich (Ti poor)	2.1	2.5	2.7		
Stoichiometric	3.3	3.8	3.9		
O poor (Ti rich)	4.0	4.4	4.6		

Ti neighbor. One could, therefore, consider these defects as a complex of the ionized donor and a host Ti atom which underwent a (4 + /3 +) charge transition (i.e., acting as an acceptor). Apparently, anatase compensates *p*-type, while rutile compensates *n*-type doping by self-trapping of the free carriers. This complementary nature of carrier self-trapping between rutile and anatase has been also shown in Ref. 60.

The data in Table II describe the energies of vertical (optical) transitions from the band edge to the defect state. Allowing for relaxation makes the adiabatic (thermal) transitions levels, ΔE^a, considerably shallower, as shown in Table III. The convergence tests show that the Γ-approximation reasonably works in the 96-atom anatase but not so well in the 72-atom rutile cell. The cell size for the latter appears to be critical (cf. also Figs. 2 and 3), but even in the former case the accuracy of the reported levels (for isolated defects) is likely to be somewhat less than the ±0.1 eV,[17] found in Group-IV semiconductors with 512-atom supercell calculations using the Γ approximation.

Experimental data are limited on dopants of TiO_2. The case of Nb seems to be well established. In rutile, Nb-doping does not cause metallic conduction even at high concentration,[21] and ultraviolet photoelectron spectroscopy (UPS) studies indicate a (vertical) transition of 0.8 eV for a Nb content corresponding to 1% of the cation sites—with energy increasing for higher concentrations.[22] Our value, calculated for 3% of the cation site, of 1.0 eV is in good agreement with that. In contrast to rutile, Nb doping turns anatase into a transparent conductive oxide (TCO),[20] without any extra feature appearing in the optical absorption spectrum.[19] Our EMT state for Nb in anatase is in line with that, and we could reproduced the observed Burnstein-Moss shift, too.[61] This shows that HSE06 works consequently well in both modifications.

The case of hydrogen is less clear from the experimental point of view. On one hand, shallow donor states have been inferred from muon spin-rotation spectra[62] for H in both rutile and anatase, while, on the other hand, a deep level transient spectroscopy (DLTS) study reported in anatase a H-related (adiabatic) charge transition level 0.5 eV below the conduction band edge.[63] Our localized polaron state with 1.0 eV vertical transition energy for H_i in rutile agrees well with the GGA + *U* result of Ref. 58, where the U parameter was determined from first principles. Decreasing the HF fraction (to 20% as in Ref. 4) does not change the localized nature of the state (increasing HF fraction prefers localization), so we believe our result for H_i to be at least qualitatively correct. (We note that the shallow state found in Ref. 64 is a likely consequence of the underestimated band gap.) The EMT state we find for H_i in anatase has an adiabatic charge transition level of 0.2 eV below the conduction band, which is shallower than the DLTS level assigned to a hydrogen-related defect.[63] We stress though that our value was obtained for a rather high concentration.

We are not aware of experimental reports on acceptor levels of Al (Ga, In, Sc, Y) in rutile or anatase. However, unlike in rutile, excitons trapped at Al have been observed in anatase, giving rise to photoluminescence (PL) below 1.7 eV.[65] This is well in line with the hole-trapping mechanism predicted by our calculation exclusively for anatase.[66] The calculated PL energy, 1.4 eV, agrees also reasonably well with the experimental value. Therefore, it seems, HSE06 is catching the right physics also for acceptors. We note that the adiabatic transition energy of Al in anatase is only 0.8 eV. What is more, the EMT state of In in rutile is about as deep as the In-bound polaron state in anatase. This is due to the high hole effective mass of rutile.[45] Because at an In concentration of 3% (of the cation sites), the level of the hole polaron shows a dispersion of 0.4 eV, *p*-type doping of anatase (with the smaller hole effective mass) is not hopeless. This is, of course, a matter of solubility.

Table IV shows the HSE06 results for the heat of formation of acceptors under various conditions (from the extreme oxygen-rich case, where the chemical potential of oxygen is equal to that in the molecule, to the oxygen-poor conditions where growth of Ti_2O_3 starts, instead of TiO_2).[23] The chemical potential of the defect (D) was set to that in its oxide, D_2O_3 . (The heat of formations was calculated in the standard way,[67] using experimental data for bulk oxides except for TiO_2.) As can be seen, the calculated heats of formation are quite large even under the most favorable (Ti-poor) conditions. However, it is well known that acceptor incorporation in TiO_2 is facilitated by the incorporation of compensating (donor-type)

oxygen vacancies.[30,68] In principle, quite high concentrations can thus be achieved, and activated subsequently by annealing in dry air and quenching. Such effects will be investigated later.

IV. CONCLUSION

We have shown that the HSE06 functional (with the standard HF fraction of 25% and screening parameter of 0.2 $Å^{-1}$) gives an improved description of the lattice parameters and the valence bandwidth of both rutile and anatase, and results in a gap that is in excellent agreement with recent GW results. Similar to the case of Group-IV semiconductors,[17] the proper description of the bulk electronic structure is accompanied by the fulfillment of the generalized Koopmans' theorem (correct dependence of the total energy on fractional occupation numbers) for host-derived defect states—independent of their shallow or deep, donor or acceptor character. The calculated charge transition levels are in good agreement with experiment for Nb in both rutile and anatase, and with the observed bound exciton in Al-doped anatase, indicating that our calculations correctly predict polaron effects, even though they are rather different in the two modifications.

The question arises, what makes HSE06 different from other corrections to standard (semi)local approximations of DFT, and to what extent is this (undoubtedly semiempirical) method reliable beyond the experimentally supported results? We find that, on the one hand, it is rather appealing to use just two common parameters for a large number of host materials with numerous defects in them—in contrast to empirical corrections (to the on-site Coulomb interaction and/or to the nonlocal part of the potential) in GGA, which have to be determined from material to material, and sometimes from defect to defect. (All the more, because, in our experience, these corrections might seriously impair ground-state properties while trying to fit the gap or achieve fulfillment of the gKT.) On the other hand, the HSE06 functional has some advantages over the other hybrids. In principle, an *ab initio* hybrid functional could be obtained by the adiabatic connection formula,[69] but there is no way of determining an *ab initio* mixing ratio in a practical two-point approximation to that by mixing GGA and HF exchange. A great number of studies on *molecules and solids* have shown that 25% HF exchange mixed with PBE[70] is best for most systems.[11,15,71] The solid-state community denotes such a hybrid as PBE0. The B3LYP hybrid differs from that by using only 20% HF exchange but introducing two additional parameters: for mixing both exchange and correlation energy from PBE and LDA. These three parameters have been determined by fitting to standard sets of *molecules* in quantum chemistry.[69] Accordingly, B3LYP does not work too well for many inorganic solids. One striking example: the *c* parameter of anatase is overestimated by 4% in B3LYP, whereas by less than 1% in HSE06. We believe that this error contributes a lot to the tendency for electron self-trapping in anatase in B3LYP calculations, despite the smaller HF fraction. The HSE functional has an additional advantage over PBE0 and B3LYP. The HF exchange is mixed only to the short-range part: up to the inverse of the screening parameter. This mimics the effect of screening, giving essentially similar results to the sX (screened exchange) functional.[72] We believe this is an essential difference to, e.g., B3LYP, which has failed the "gKT test."[8] The consistently good performance of HSE06 in the gKT test is the basis of our trust in this method but, even two (or, for that matter, one) empirical parameters make a method semiempirical. Therefore, transferability has to be checked, as we did here and in Ref. 17. However, because there is no practically feasible *ab initio* theoretical method to calculate defects in TiO_2, HSE06 seems to us to be the best choice. The agreement with the scarce experimental data on defects in TiO_2 supports this conclusion.

ACKNOWLEDGMENTS

Support of the Supercomputer Center of Northern Germany (HLRN Grant No. hbc00001) is highly appreciated. The authors are grateful to S. Lany for many helpful discussions and for the help with the charge corrections.

*deak@bccms.uni-bremen.de

[1] W. R. L. Lambrecht, in *Advanced Calculations for Defects in Materials*, edited by A. Alkauskas, P. Deák, J. Neugebauer, A. Pasquarello, and C. G. Van de Walle (Wiley-VCH, Berlin 2011), p. 359.
[2] S. Lany and A. Zunger, Phys. Rev. B **78**, 235104 (2008).
[3] S. Lany and A. Zunger, Phys. Rev. B **81**, 113201 (2010).
[4] A. Janotti, J. B. Varley, P. Rinke, N. Umezawa, G. Kresse, and C. G. Van de Walle, Phys. Rev. B **81**, 085212 (2010).
[5] G. Pacchioni, F. Frigoli, D. Ricci, and J. A. Weil, Phys. Rev. B **63**, 054102 (2000); O. F. Schirmer, J. Phys. Condens. Matter **18**, R667 (2206); A. M. Stoneham, J. Gavartin, A. L. Shluger, A. V. Kimmel, D. Muñoz Ramo, H. M. Rønnow, G. Aeppli, and C. Renner, *ibid.* **19**, 255208 (2007).
[6] S. Lany and A. Zunger, Phys. Rev. B **80**, 085202 (2009); S. Lany, in *Advanced Calculations for Defects in Material* (Ref.1), p. 183.
[7] B. J. Morgan and G. W. Watson, Phys. Rev. B **80**, 233102 (2009).
[8] F. Bruneval, Phys. Rev. Lett. **103**, 176403 (2009).
[9] C.-O. Almbladh and U. von Barth, Phys. Rev. B **31**, 3231 (1985).
[10] J. Robertson, K. Xiong, and S. J. Clark, Phys. Status Solidi B **243**, 2054 (2006).
[11] J. Heyd, G. E. Scuseria, and M. Ernzerhof, J. Chem. Phys. **118**, 8207 (2003); A. V. Krukau, O. A. Vydrov, A. F. Izmaylov, and G. E. Scuseria, *ibid.* **125**, 224106 (2006).
[12] P. Broqvist, A. Alkauskas, and A. Pasquarello, Phys. Rev. B **80**, 085114 (2009).
[13] X. Wu, A. Selloni, and R. Car, Phys. Rev. B **79**, 085102 (2009).
[14] A. Janotti, and C. G. Van de Walle, in *Advanced Calculations for Defects in Materials* (Ref. 1), p. 139.
[15] M. Marsman, J. Paier, A. Stroppa, and G. Kresse, J. Phys.: Condens. Matter **20**, 064201 (2008).
[16] J. L. Lyons, A. Janotti, and C. G. Van de Walle, Appl. Phys. Lett. **95**, 252105 (2009).
[17] P. Deák, B. Aradi, T. Frauenheim, E. Janzén, and A. Gali, Phys. Rev. B **81**, 153203 (2010); P. Deák, A. Gali, B. Aradi, and T. Frauenheim, in *Advanced Calculations for Defects in Materials* (Ref. 1). p. 139.

[18]For references see the Description of the International CECAM workshop (Bremen 2010) on Titania, [http://www.bccms.uni-bremen.de/index.php?id = 1839].
[19]D. D. Mulmi, T. Sekiya, N. Kamiya, S. Kurita, Y. Murakami, and T. Kodaira, J. Phys. Chem. Solids **65,** 1181 (2004).
[20]Y. Furubayashi, T. Hitosugi, Y. Yamamoto, K. Inaba, G. Kinoda, Y. Hirose, T. Shimada, and T. Hasegawa, Appl. Phys. Lett. **86**, 252101 (2005).
[21]S. X. Zhang, D. C. Kundaliya, W. Yu, S. Dhar, S. Y. Young, L. G. Salamanca-Riba, S. B. Ogale, R. D. Vispute, and T. Venkatesan, J. Appl. Phys. **102**, 013701 (2007).
[22]D. Morris, Y. Dou, J. Rebane, C. E. J. Mitchell, R. G. Egdell, D. S. L. Law, A. Vittadini, and M. Casarin, Phys. Rev. B **61**, 13445 (2000).
[23]J. Osorio-Guillén, S. Lany, and A. Zunger, Phys. Rev. Lett. **100**, 036601 (2008).
[24]B. J. Morgan, D. O. Scanlon, and G. W. Watson, J. Mater. Chem. **19**, 5175 (2009).
[25]N. Orita, Jpn. J. Appl. Phys., Part 1 **49**, 055801 (2010).
[26]C. Di Valentin, G. Pacchioni, and A. Selloni, J. Phys. Chem. C **113**, 20543 (2009).
[27]G. Mattioli, F. Filippone, P. Alippi, and A. Amore Bonapasta, Phys. Rev. B **78**, 241201 (2008).
[28]E. Finazzi, C. Di Valentin, G. Pacchioni, and A. Selloni. J. Chem. Phys. B **129**, 154113 (2008).
[29]R. Asahi, T. Morikawa, T. Ohwaki, K. Aoki, and Y. Taga, Science **293**, 269 (2001).
[30]C. Di Valentin, E. Finazzi, G. Pacchioni, A. Selloni, S. Livraghi, M. C. Paganini, and E. Giamello, Chem. Phys. **339**, 44 (2007); C. Di Valentin, E. Finazzi, G. Pacchioni, A. Selloni, S. Livraghi, A. M. Czoska, M. C. Paganini, and E. Giamello, Chem. Mater. **20**, 3706 (2008).
[31]R. Long and N. J. English, Appl. Phys. Lett. **94**, 132102 (2009); R. Long and N. J. English, Chem. Phys. Lett. **478**, 175 (2009).
[32]W. Zhu *et al*., Phys. Rev. Lett. **103**, 226401 (2009).
[33]Y. Gai, J. Li, Sh.-Sh. Li, J.-B. Xia, and S.-H. Wei Phys. Rev. Lett. **102**, 036402 (2009).
[34]U. Gesenhues, J. Photochem. Photobiol. A **139**, 243 (2001).
[35]M. Steveson, T. Bredow, and A. Gerson, Phys. Chem. Chem. Phys. **4**, 358 (2002).
[36]M. M. Islam, T. Bredow, and A. Gerson, Phys. Rev. B **76**, 045217 (2007).
[37]A. Stashans and S. Bermeo, Chem. Phys. **363**, 100 (2009).
[38]R. Shirley, M. Kraft, and O. R. Inderwildi, Phys. Rev. B **81**, 075111 (2010).
[39]G. Kresse and J. Hafner, Phys. Rev. B **49**, 14251 (1994); G. Kresse and J. Furthmüller, *ibid*. **54**, 11169 (1996); G. Kresse and D. Joubert, *ibid*. **59**, 1758 (1999).
[40]H.J. Monkhorst and J.K. Pack, Phys. Rev. B **13**, 5188 (1976).
[41]J. Paier, M. Marsman, K. Hummer, G. Kresse, I.C. Gerber, and J.G. Angyan, J. Chem. Phys. **124**, 154709 (2006).
[42]M. Giarola, A. Sanson, F. Monti, G. Mariotto, M. Bettinelli, A. Speghini, and G. Salviulo, Phys. Rev B **81**, 174305 (2010).
[43]The lattice parameters have been determined to an accuracy of no better than 1%, and this introduces an additional error source of less than 0.1 eV into the supercell results on defects.
[44]M. Mikami, S. Nakamura, O. Kitao, H. Arakawa, and X. Gonze, Jpn. J. Appl. Phys., Part 2 **39**, L847 (2000).
[45]W. Kang and M. S. Hybertsen, Phys. Rev. B **82**, 085203 (2010).
[46]L. Chiodo, J. M. García-Lastra, A. Iacomino, S. Ossicini, J. Zhao, H. Petek, and Angel Rubio, Phys. Rev. B **82**, 045207 (2010).
[47]M. van Schilfgaarde, T. Kotani, and S. Faleev, Phys. Rev. Lett. **96**, 226402 (2006).
[48]L. Thulin and J. Guerra, Phys. Rev. B **77**, 195112 (2008).
[49]Note that G_0W_0 calculations within the plasmon pole approximation give higher gap values than the one obtained with the frequency dependence taken fully into account. See Ref. 46.
[50]Y. Tezuka, S. Shin, T. Ishii, T. Ejima, S. Suzuki, and S. Sato, J. Phys. Soc. Jpn., Part 1 **63**, 347 (1994).
[51]P. Deák, B. Aradi, and T. Frauenheim, J. Phys. Chem. C **115,** 3443 (2011).
[52]J. Muscat, V. Swamy, and N. M. Harrison, Phys. Rev. B **65,** 224112 (2002).
[53]H. Tang, F. Lévy, H. Berger, and P. E. Schmid, Phys. Rev. B **52**, 7771 (1995).
[54]J. Pascual, J. Camassel, and H. Mathieu, Phys. Rev. B **18**, 5606 (1978).
[55]R. Sanjinés, H. Tang, H. Berger, F. Gozzo, G. Margaritono, and F. Lévy, J. Appl. Phys. **75**, 2945 (1994).
[56]We note that no distinct defect levels arise in case of EMT states. The vertical charge transition energy was determined from the shift of the band edge (after potential alignment). In the case of the localized states the weighted average at the *k* points of the MP set was taken.
[57]C. Freysoldt, J. Neugebauer, and C. G. Van de Walle, Phys. Rev. Lett. **102**, 016402 (2009). *Advanced Calculations for Defects in Materials*, A. Alkauskas, P. Deák, J. Neugebauer, A. Pasquarello, and C. G. Van de Walle (Wiley-VCH, Berlin, 2011), p. 241.
[58]F. Filippone, G. Mattioli, P. Alippi, and A. Amore Bonapasta, Phys. Rev. B **80**, 245203 (2009).
[59]M. V. Koudriachova, S. W. de Leeuw, and N. M. Harrison, Phys. Rev. B **70**, 165421 (2004).
[60]S. Lany and A. Zunger (unpublished).
[61]H. A. Huy, B. Aradi, T. Frauenheim, and P. Deák, Phys. Rev. B **83**, 155201 (2011).
[62]S. F. J. Cox, J. L. Gavartin, J. S. Lord, S. P. Cottrell, J. M. Gil, H. V. Alberto, J. Piroto Duarte, R. C. Vilao, N. Ayres de Campos, D. J. Keeble, E. A. Davis, M. Charlton, and D. P. van der Werf, J. Phys. C: Condens. Matter. **18**, 1079 (2006).
[63]T. Miyagi, M. Kamei, T. Mitsuhashi, and A. Yamazaki, Appl. Phys. Lett. **88**, 132101 (2006).
[64]K. Xiong, J. Robertson, and S. J. Clark, J. Appl. Phys. **102**, 083710 (2007).
[65]H. Tang, H. Berger, P.E. Schmid, and F. Lévy, Solid State Commun. **87**, 847 (1993).
[66]NB: Al in TiO_2 is always compensated by oxygen vacancies, so Al is negatively charged in equilibrium.
[67]C. G. Van de Walle and J. Neugebauer, J. Apppl. Phys. **95**, 3851 (2004).
[68]Y. Yan and S.-H. Wei, Phys. Status Solidi B **245**, 641 (2008).
[69]A. D. Becke, J. Chem. Phys. **98**, 5648 (1993).
[70]J. P. Perdew, K. Burke, and M. Ernzerhof, Phys. Rev. Lett. **77**, 3865 (1996).
[71]J. P. Perdew, M. Ernzerhof, and K. Burke, J. Chem. Phys. **105**, 9982 (1996).
[72]S. J. Clarke and J. Robertson, in Advanced Calculations for Defects in Materials (Ref.1), p. 79.